



**UNIVERSITATEA
BABEȘ-BOLYAI**



Faculty of Chemistry and Chemical Engineering

Department of Chemistry

Supramolecular Organic and Organometallic Chemistry Centre

PhD thesis summary

**TRIORGANOPNICTOGEN(V) DI[(ISO)NICOTINATES] AND THEIR
IMPLICATIONS IN COORDINATION POLYMER CHEMISTRY**

Ahmad Ben Kiran

**Scientific advisor:
Acad. Cristian SILVESTRU**

Cluj-Napoca

2024

Review committee

PRESIDENT

Prof. Dr. habil. ing. Tiberiu FRENȚIU
Babeș-Bolyai University, Cluj-Napoca, Romania

SCIENTIFIC ADVISOR

Acad. Cristian SILVESTRU
Babeș-Bolyai University, Cluj-Napoca, Romania

REVIEWERS

Conf. Dr. Vlad CHIRIAC
Western University of Timișoara, Timișoara, Romania

Conf. Dr. Augustin MĂDĂLAN
University of Bucharest, Bucharest, Romania

Conf. Dr. ing. Monica VENTER
Babeș-Bolyai University, Cluj-Napoca, Romania

Table of Contents

1. Aim of these studies	7
2. Triorganopnictogen(V) carboxylates	7
2.1. General introduction	7
2.2. Literature data	9
3. Coordination polymers	26
3.1. General introduction	26
3.2. Single crystal X-ray diffraction	26
Reaction with AgClO₄	26
Reaction with AgOTf	28
Reaction with (Ph₃P)₂Cu(ClO₄):	31
Reaction with Hg(SCN)₂:	32
Reaction with Hg(CN)₂:	33
Reaction with Hg(CN)₂:	34
4. Conclusion.....	35

Key-words: Coordination polymers, triorganobismuth(V) dicarboxylates, triorganoantimony(V) dicarboxylates, organometallic spacers, secondary interactions, concentration dependent chemical shift, concentration dependent coupling constant, crystal engineering.

1. Aim of these studies

3,3'-Bipyridine and 4,4'-bipyridine (Figure 1) display terminal N,N' ditopic divergent donor sites enabling them to form coordination chains with linear topologies and are widely used in supramolecular chemistry.



Figure 1. 3,3'-bipyridine (left) and 4,4'-bipyridine (right).

The main goal of this work is the synthesis of new and known triorganoantimony(V) and triorganobismuth(V) dicarboxylates, *i.e.* using nicotinate and iso-nicotinate groups (Figure 2), thus displaying similar donor sites to those of the tecton archetypes mentioned above. The capability of these organometallic compounds to act as ditopic (μ) bridging spacers in coordination polymers will be tested.



Figure 2. isonicotinate group (left) and nicotinate group (right).

2. Triorganopnictogen(V) carboxylates

2.1. General introduction

Antimony is known since antiquity as it was proved by archeologists. By the means of radioactive dating of several artifacts, it was shown that antimony was used in ancient Egypt as a glass pigment under the form of lead antimonate ($\text{Pb}_2\text{Sb}_2\text{O}_7$).¹ Historians also found evidence that this metal was first isolated in its elemental form in the 16th century by Italian metallurgist Vannoccio Biringuccio.² It is the fourth element of group 15, “the pnictogen group”, within the main group elements of the periodic table (p block). This element has two main natural stable isotopes ^{121}Sb (57.21%) and ^{123}Sb (42.79%). It exhibits in most compounds two common stable oxidation states, *i.e.* +3 and +5, due to its electronic configuration $[\text{Kr}]4d^{10}5s^25p^3$. Antimony is mostly found as stibnite ores (Sb_2S_3), main source of this metal, and rarely in

¹ A. J. Shortland, *Archeometry*, **2006**, 48(4), 657-669.

² V. Biringuccio, *De la pirotechnia*, **1540**, 2, 3.

its elemental form Sb(0) in metal-bearing siliceous gangue along other antimony, gold and silver ores.³ As for its applications, by the year 2000, usage of nearly 60% of antimony-containing products was directed toward flame retardant materials, while 10% and 9% of antimony compounds was used as catalyst and plastic stabilizer, or in pigments, respectively.⁴ Antimony based compounds are also found to be used in medicine, predominantly in the treatment of the tropical diseases, *e.g. Leishmaniasis*. The active ingredients in such drugs include sodium stibogluconate (Pentostam) and meglumine antimonate (Glucantime).⁵

The name of the heavier pnictogen, *i.e. bismuth*, was found to be mentioned for the first time in the 1450s but was recognized as a distinct element only from the mid-18th century by French chemist Claude Francois Geoffroy. This element has a $[\text{Xe}]4f^{14}5d^{10}6s^26p^3$ ground state electronic configuration which generates two common stable oxidation states: +3 and +5. In nature, bismuthinite (Bi_2S_3) and bismite (Bi_2O_3) are the main ores of bismuth with a naturally occurring stable isotope ^{209}Bi (100%); this element also has several stable synthetic isotopes with a long half-life time like ^{207}Bi , ^{208}Bi and ^{210}Bi . Despite being a heavy metal and the element with the most metallic character in its group, it also has similar behavior and properties to insulators and semi-conductors of other main group elements.⁶ This main group element is also valued in the drug industry due to its effective healing and prevention abilities against gastric and duodenal ulcer through colloidal bismuth subcitrate (*De-Nol*) and bismuth subsalicylate (*Pepto-Bismol*).⁵

In the +3 oxidation state, antimony and bismuth both usually need their $5p$ or $6p$ orbitals, respectively, for bonding; while an sp^3 hybridization can be usually considered for antimony, for the heavier pnictogen, bismuth, the non-bonding pair of electrons is left in the $6s$ orbital. Compounds SbX_3 and BiX_3 adopt a trigonal pyramidal geometry with X-Pn-X angle value ranging between 90° and 100° ($\text{Pn} = \text{Sb, Bi}$). Even in oxidation state +3 the d orbitals are often used, resulting in an increase of coordination number at the metal center. In the case of the +5 oxidation state, the metal centers are usually sp^3d hybridized adopting a trigonal bipyramidal geometry.

³ S. C. Grund, K. Hanusch, H. J. Breunig, H. U. Wolf, *Antimony and Antimony Compounds*, Ullmann's Encyclopedia of Industrial Chemistry, Wiley-VCH, Weinheim, **2006**.

⁴ W. C. Butterman, J. F. Carlin, Jr., *Mineral Commodity Profiles: Antimony*, **2004**, 03-019.

⁵ E. R. T. Tiekink, *Crit. Rev. Oncol. Hematol.*, **2002**, *42*, 217-224.

⁶ H. Suzuki, N. Komatsu, T. Ogawa, T. Murafuji, T. Ikegami, Y. Matano, *Organobismuth Chemistry*, Elsevier, Kyoto, **1999**.

2.2. Literature data

This chapter is dedicated to present literature data of compounds sharing similarities to triorganopnictogen(V) carboxylates further discussed in this work. Synthetic pathways, characterization and description of the metal core and supramolecular assemblies of these $R_3Pn[O(O)CR']_2$ ($Pn = Sb, Bi$) are the focal point of the discussion. This class of compounds is known, reported and extensively studied since the last century.

The first trimethylantimony(V) dicarboxylate was reported in 1966 by the Shindo's group to elucidate the nature of the Sb–O bond *via* IR spectroscopy,⁷ while triphenylantimony(V) dicarboxylates were first reported by the Challenger's group in 1927.⁸ Triphenylbismuth(V) dicarboxylates were also reported for the first time by the above-mentioned Challenger's group in the same article in 1927,¹³ while the first structure of a triorganobismuth(V) dicarboxylate wasn't reported until the late '80s.⁹

2.3. Original contribution

$R_3E(O_2R')_2$ compounds are well known and studied but none used as spacers for the generation of coordination polymers. Me_3SbBr_2 was obtained through oxidation of *in situ* prepared Me_3Sb (from $MeMgI$ and $SbCl_3$, in diethyl ether) with Br_2 in CCl_4 , under inert atmosphere [Scheme 2, equation (2)].¹⁰ While the derivatives Ph_3SbCl_2 and R_3BiCl_2 ($R = Ph, p\text{-Tol}$) were obtained according to literature methods by oxidation of the corresponding triorganopnictogens with SO_2Cl_2 in CH_2Cl_2 [Scheme 2, equation (3)].¹¹

The triorganopnictogen(V) dicarboxylates **1** – **7** were obtained following a modified synthetic pathway found in the literature,¹² by reacting the triorganobismuth dichloride, triphenylantimony dichloride and trimethylantimony dibromide with the respective alkali metal carboxylate salt in EtOH as shown in Schemes 3 - 6 below.

⁷ M. Shindo, R. Okawara, *J. Organomet. Chem.*, **1966**, 5, 537-544.

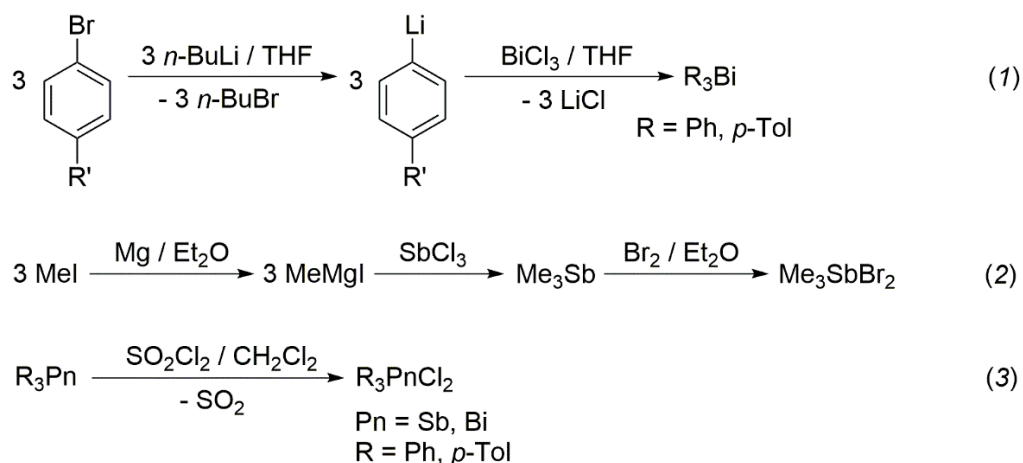
⁸ F. Challenger, V. K. Wilson, *J. Chem. Soc.*, **1927**, 209-213.

⁹ M. Domagala, H. Preut, F. Huber, *Acta Crystallogr., Sect. C: Struct. Chem.*, **1988**, C44, 830-832.

¹⁰ M. Wieber, M. Mirbach, *Sb – Organoantimony Compounds, Part 4*, in *Gmelin Handbuch of Inorganic Chemistry*, Springer, Berlin, **1986**, 60-70.

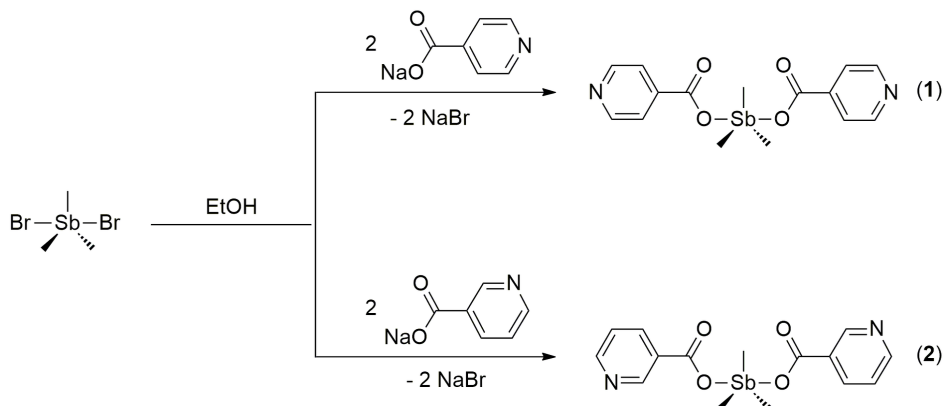
¹¹ A. F. M. Mustafizur Rahman, T. Murafuji, M. Ishibashi, Y. Miyoshi, Y. Sugihara, *J. Organomet. Chem.*, **2005**, 690, 4280-4284.

¹² M. I. Ali, M. K. Rauf, A. Badshah, I. Kumar, C. M. Forsyth, P. C. Junk, L. Kedzierski, P. C. Andrews, *Dalton Trans.*, **2013**, 42, 16733-16741.



Scheme 2. Synthetic pathway followed to obtain triphenylbismuth, triphenylbismuth dichloride, triphenylantimony dichloride and Me₃SbBr₂.

Compounds **1-2**, which have already been reported in the literature,¹³ were identified using ¹H NMR spectroscopy. While the Ph₃Sb[O(O)CC₅H₄N-3]₂ (**3**) derivative was obtained in a similar high yield (96%) as reported previously (*i.e.* 99%) using the alternative method based on treatment of the Ph₃Sb / carboxylic acid mixture in Et₂O with an aqueous solution of hydrogen peroxide.¹⁴ The new triorganobismuth(V) dicarboxylates, R₃Bi[O(O)CC₅H₄N-4]₂ and R₃Bi[O(O)CC₅H₄N-3]₂ (R = Ph,¹⁵ *p*-Tol), were obtained in good yields using a preformed alkali metal carboxylate (Schemes 6 and 7), they were characterized *via* multinuclear (¹H and ¹³C) NMR aided by bidimensional (COSY, HSQC and HMBC) NMR in order to assign the respective resonances. All measurements were performed in CDCl₃ at room temperature.



Scheme 3. Synthesis of trimethylantimony diisonicotinate (**1**) and trimethylantimony dinicotinate.

¹³ N. S. Tóth, Organoantimony(V) carboxylates – spacers for coordination polymers. B.Sc. Thesis, Babeş-Bolyai University, 2015.

¹⁴ V. V. Sharutin, O. K. Sharutina, A. P. Pakusina, T. P. Platonova, V. V. Zhidkov, M. A. Pushilin, A. V. Gerasimenko, *Russ. J. Coord. Chem.*, **2003**, 29(10), 694-702.

¹⁵ A. Ben Kiran, T. Mocanu, A. Pöllnitz, S. Shova, M. Andruh, C. Silvestru, *Dalton Trans.*, **2018**, 47, 2531-2542.

For compounds **1** and **2**, the aliphatic region of the ^1H NMR spectrum showed that a change in the chemical shift of the methyl group's protons had occurred with $\delta_{\text{Me}} = 2.09$ (compound **1**) and $\delta_{\text{Me}} = 2.1$ ppm (compound **2**) shifting downfield from $\delta_{\text{Me}} = 2.63$ ppm (Me_3SbBr_2) indicating the consumption of the entirety of the starting material, as depicted in Figure 3 below. This difference in value is due to the change of the antimony's anion, provoking an alteration to the electron density around the protons' nucleus.

The appearance of two chemical shifts in the aromatic region: H_4 ($\delta_{\text{H}_4} = 7.77\text{-}7.78$ ppm) and H_5 ($\delta_{\text{H}_5} = 8.72\text{-}8.74$ ppm) for compound **1** and four chemical shifts in the aromatic region: H_{4-7} ($\delta_{\text{H}_4} = 9.16$, $\delta_{\text{H}_5} = 8.71\text{-}8.73$, $\delta_{\text{H}_6} = 7.33\text{-}7.37$ and $\delta_{\text{H}_7} = 8.23\text{-}8.25$ ppm) for compound **2** with 4:9 and 2:9 integration ratio relative to the methyl group, respectively, indicates the presence of the target compounds at the end of the reactions. It is worth mentioning that nicotinic, iso-nicotinic acid and their alkali salts are insoluble in CDCl_3 , their NMR analysis is usually performed in D_2O , thus the appearance of the expected four signals of the nicotinate group and two signals for iso-nicotinate moiety in the aromatic region of the ^1H NMR in CDCl_3 , adds proof to the target compounds' presence.

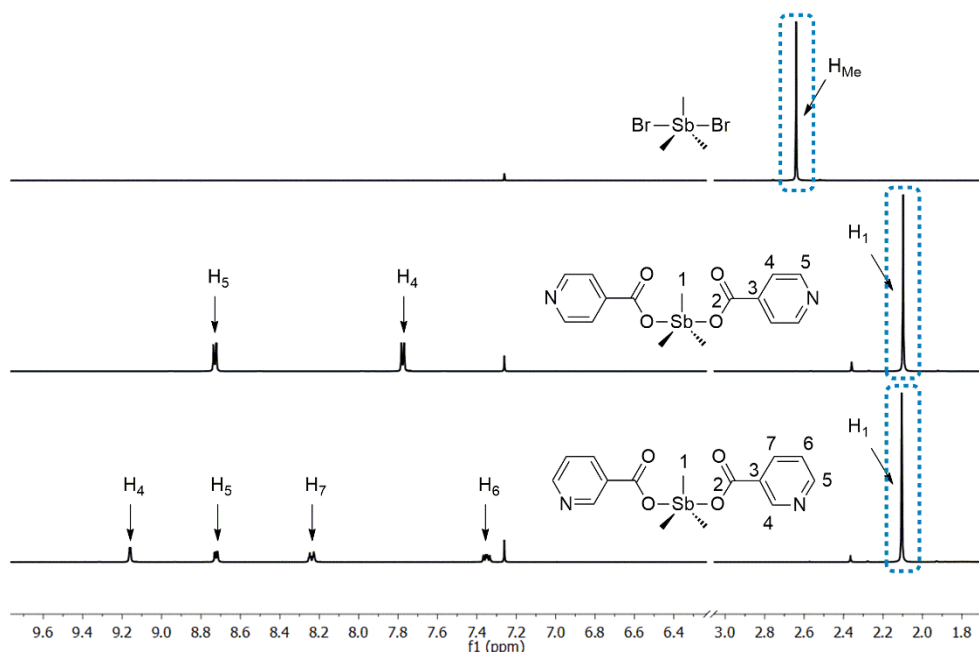
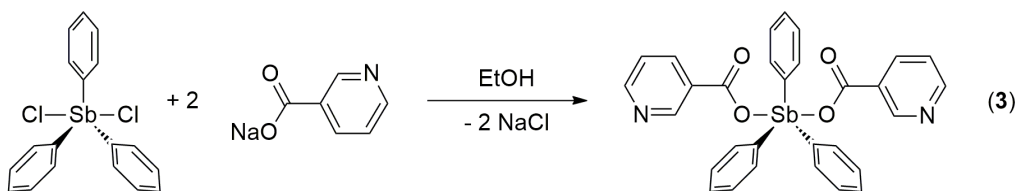


Figure 3. Details of the stacked ^1H NMR spectra (CDCl_3 , 400 MHz) of the starting material (top), compounds **1** (middle) and **2** (bottom).



Scheme 4. Synthesis of triphenylantimony dinicotinate (**3**).

The ^1H NMR analysis recorded for compound **3** shows six signals in the aromatic area (Figure 4), where the chemical shifts of the hydrogen atoms from the phenyl moiety attributed to H_{3-4} are overlapped at 7.53 ppm and H_2 's chemical shift almost eclipses H_8 at 8.10-8.15 ppm. The attribution of the chemical shifts of the heteroaromatic ring's hydrogen and carbon atoms followed a similar correlation used with compounds **4** and **5** as will be mentioned later on.

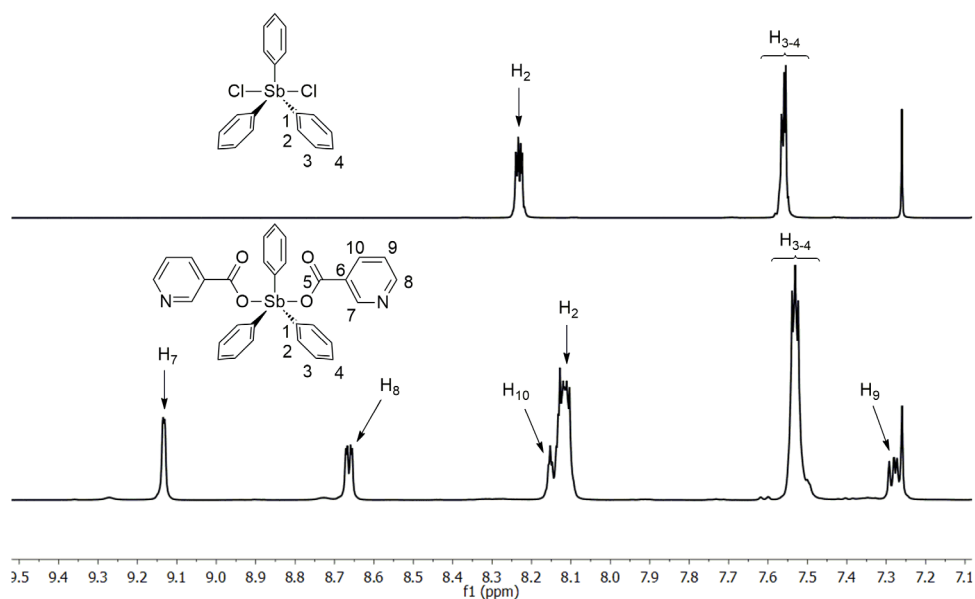
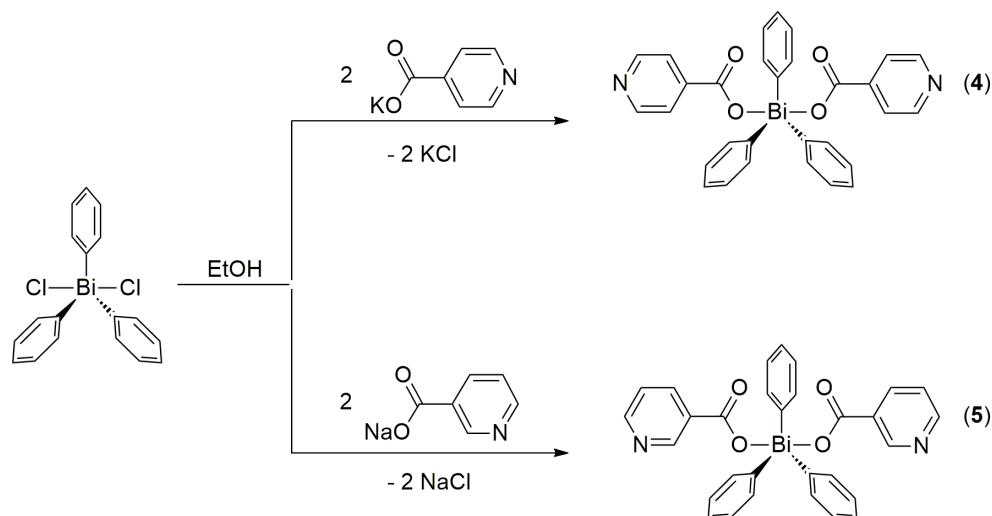


Figure 4. Stacked ^1H NMR spectra (CDCl_3 , 400 MHz) of the aromatic region of the starting material (top) and compound **3** (bottom).



Scheme 5. Synthesis of triphenylbismuth diisonicotinate (**4**) and triphenylbismuth dinicotinate (**5**).

For compounds **4** and **5**, the ^1H NMR spectra recorded revealed the expected number of signals: five chemical shifts in the aromatic region for compound **4** with $\delta_{\text{H}4} = 7.51$ ppm, $\delta_{\text{H}3} = 7.64$ ppm, $\delta_{\text{H}2} = 8.27$ ppm for the phenyl group and $\delta_{\text{H}7} = 7.74$ ppm, $\delta_{\text{H}8} = 8.64$ ppm for the heteroaromatic ring, while seven chemical shifts for **5** with $\delta_{\text{H}4} = 7.49$ ppm, $\delta_{\text{H}3} = 7.63$ ppm, $\delta_{\text{H}2} = 8.3$ ppm for the phenyl moiety and $\delta_{\text{H}9} = 7.26$ ppm, $\delta_{\text{H}10} = 8.2$ ppm, $\delta_{\text{H}8} = 8.63$ ppm, $\delta_{\text{H}7} = 9.15$ ppm for the nicotinic group (Figure 5). Only slight changes were observed to the chemical shifts of the *para* and *meta* hydrogen atoms from the phenyl rings between reagent and products except for those in the *ortho* position, shifting from $\delta_{\text{H}2} = 7.49$ ppm (Ph_3BiCl_2) to $\delta_{\text{H}2} = 8.27$ ppm (compound **4**) and $\delta_{\text{H}2} = 8.2$ ppm (compound **5**). This is due to the change in electronegativity and environment surrounding the phenyl moieties from dichloride to dicarboxylate. It is clear that a resonance pattern emerges in the ^1H NMR spectra regarding the heteroaromatic rings for similar carboxylate compounds, therefore their assignment will be discussed exclusively for compounds **4** and **5**.

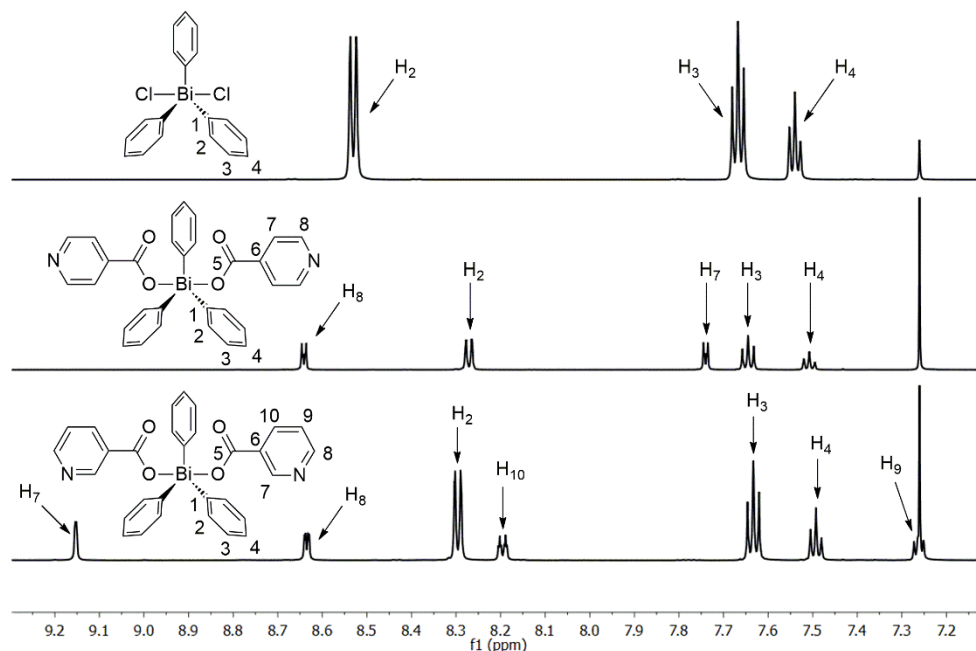


Figure 5. Stacked ^1H NMR spectra (CDCl_3 , 400 MHz) of the aromatic region of the starting material (top), compounds **4** (middle) and **5** (bottom).

The X-ray structures of both **2** and **3** were reported and show that the antimony cores adopt a typical trigonal bipyramidal geometry,^{13,14} where the oxygen atoms of the carboxylic groups hold the axial positions while the carbon atoms of aliphatic or aromatic groups hold the equatorial positions.

X-ray diffraction studies on the suitable crystals obtained of both compounds **4** and **5** show that their bismuth core adopt an expected trigonal bipyramidal geometry, with the carbon atoms of the phenyl groups filling the three equatorial positions and the oxygen atoms from the carboxylate fragments occupying the two apical positions. The linearity of the divergent donor sites is attributed to the axial position of the carboxylate groups in the antimony and bismuth coordination sphere. All organopnictogen(V) carboxylates prepared have a rigid backbone with pyridyl moieties displaying a degree of freedom with respect to the adopted conformation. Another common structural aspect is the fact that in the case of **4** and **5**, both aromatic and heteroaromatic rings are engaged in hydrogen bonding and π - π stacking to sustain the supramolecular architecture. The ORTEP-like diagrams are depicted respectively in Figures 6 and 7.

Compound **4** crystallizes in the orthorhombic space group $P 2_1/n$. The suitable crystals for X-ray measurement were obtained *via* slow diffusion of water vapor on a solution of **4** in DMSO and no solvent was found in the final structure.

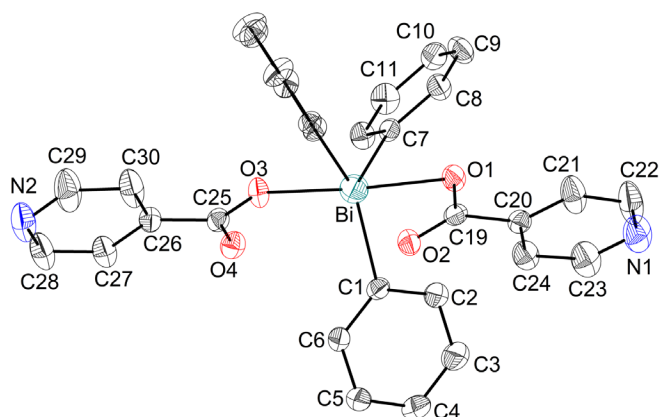


Figure 6. ORTEP representation of the molecular structure of $(C_6H_5)_3Bi(O_2CC_5H_4N-4)_2$ (**4**) showing 30% probability displacement ellipsoids and the atom numbering scheme (hydrogen atoms were omitted for clarity).

Compound **5** crystallizes in the triclinic space group $p\bar{1}$. Suitable crystals for X-ray measurement were obtained *via* slow diffusion of hexane on a solution of **5** in $CHCl_3$ and no solvent was found taking part in the final supramolecular structure.

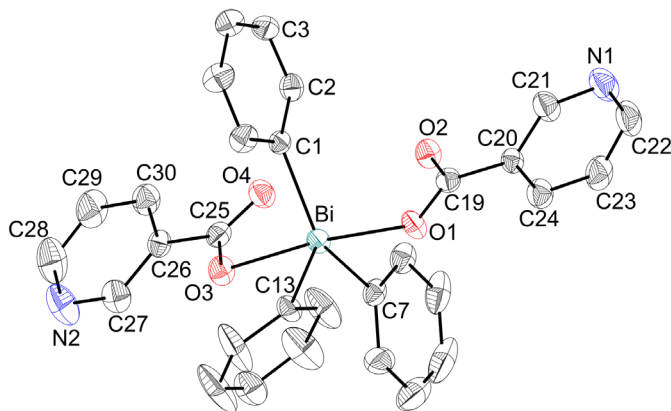
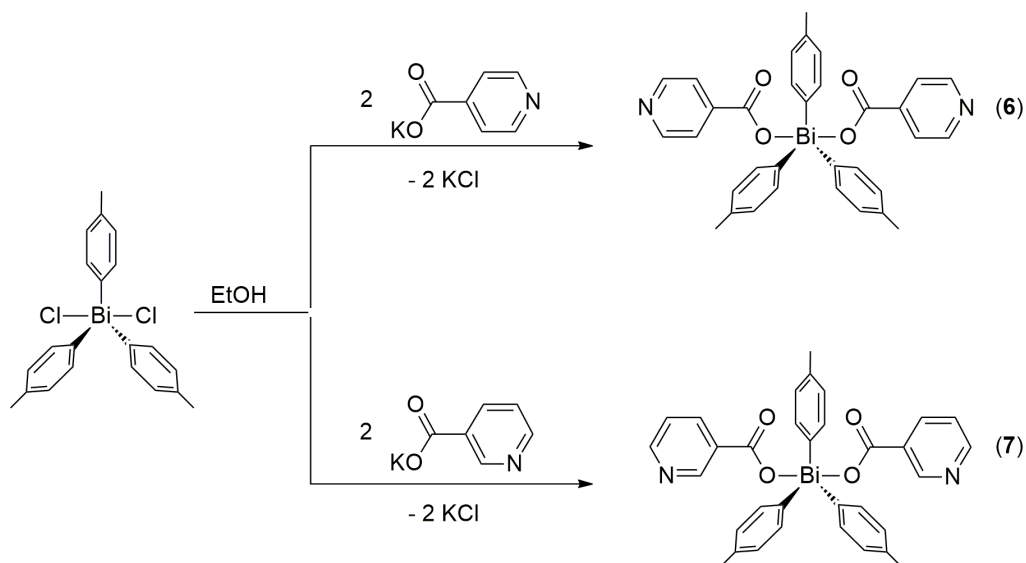


Figure 7. ORTEP representation of the molecular structure of $(C_6H_5)_3Bi(O_2CC_5H_4N-3)_2$ (**5**) showing 30% probability displacement ellipsoids and the atom numbering scheme.



Scheme 6. Synthesis of tri-*p*-tolylbismuth diisonicotinate (**6**) and tri-*p*-tolylbismuth dinicotinate (**7**).

For compounds **6** and **7**, a slight downfield shift was observed in the aliphatic region for the hydrogen atoms of the methyl groups of the *p*-tolyl moiety from $\delta_{\text{Me}} = 2.41$ ppm ($\text{p-tol}_3\text{BiCl}_2$) to $\delta_{\text{Me}} = 2.39$ ppm (compound **6**) and $\delta_{\text{Me}} = 2.38$ ppm (compound **7**). In the aromatic region, the expected four peaks appeared for **6**: two peaks for the *p*-tolyl group at $\delta_{\text{H}_3} = 7.43$ ppm and $\delta_{\text{H}_2} = 8.12$ ppm and two peaks for the heteroaromatic fragment at $\delta_{\text{H}_7} = 7.73$ ppm and $\delta_{\text{H}_8} = 8.63$ ppm, while six peaks were recorded for **7**: two peaks for the *p*-tolyl group at $\delta_{\text{H}_3} = 7.42$ ppm and $\delta_{\text{H}_2} = 8.15$ ppm with four peaks for the heteroaromatic ring at $\delta_{\text{H}_{10}} = 7.26$ ppm (shadowing the CDCl_3 peak), $\delta_{\text{H}_{11}} = 8.19$ ppm, $\delta_{\text{H}_9} = 8.63$ ppm and $\delta_{\text{H}_8} = 9.14$ ppm, as presented in Figure 8.

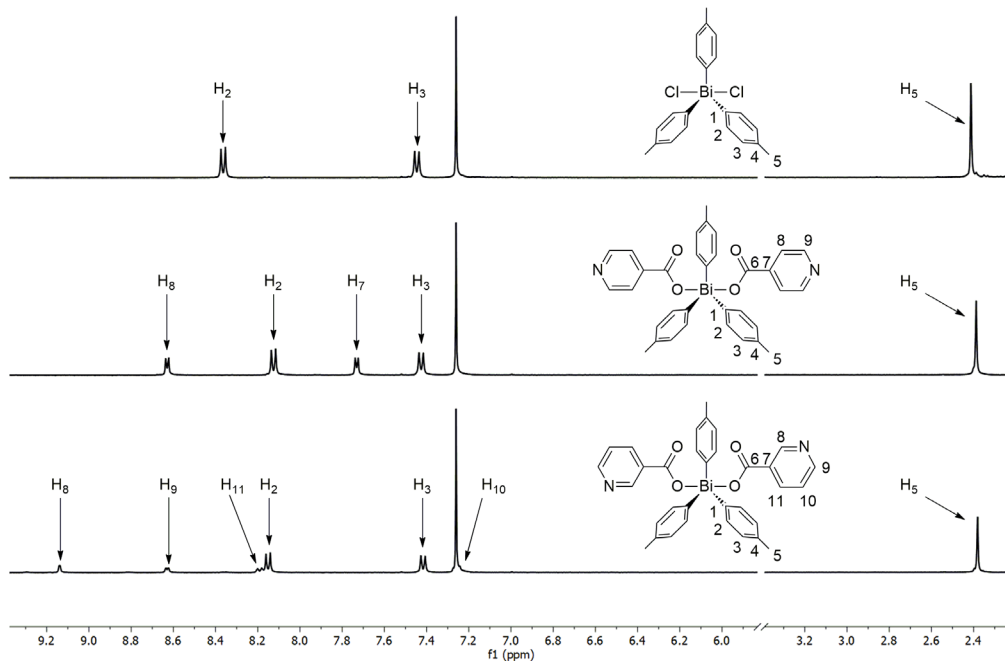


Figure 8. Details of the stacked ¹H NMR spectra (CDCl₃, 400 MHz) of starting material (top), compounds **6** (middle) and **7** (bottom).

Compound **6** crystallizes in the P-1 space group and single crystals suitable for x-ray diffraction analysis were obtained from the washing hexane solution. No solvent was found to take part in the final structure (Figure 9).

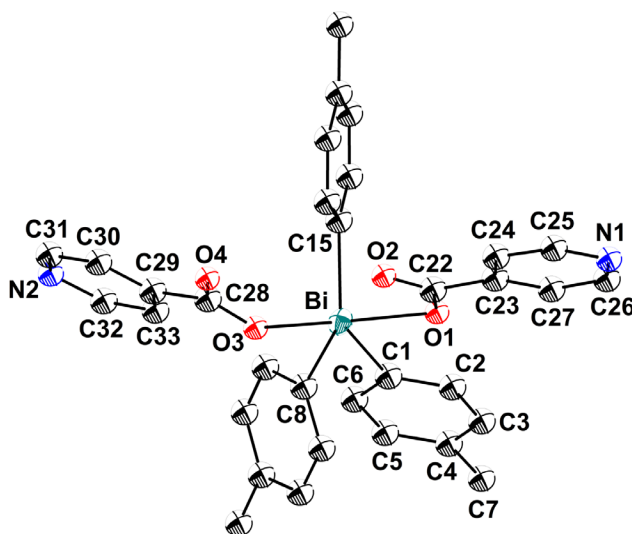
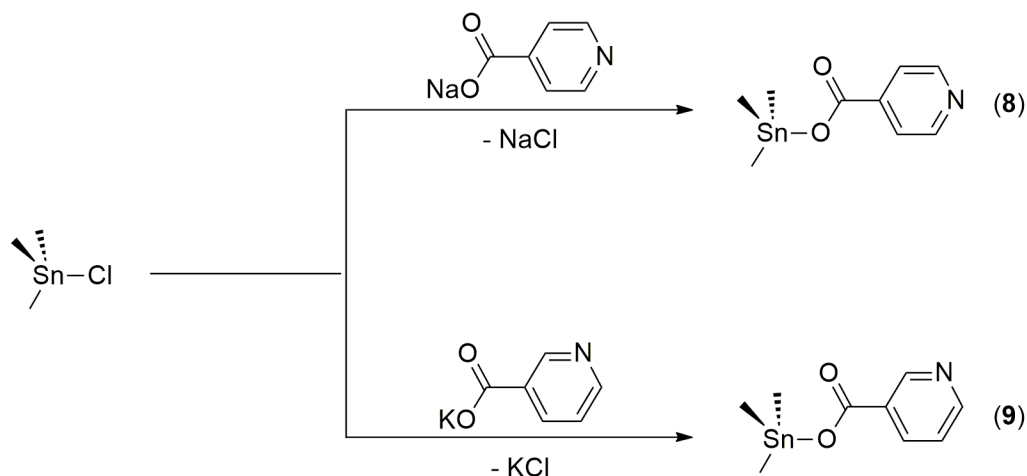


Figure 9. ORTEP representation of the molecular structure of [C₆H₅(CH₃)-4]₃Bi(O₂CC₅H₄N-3)₂ (**6**) showing 30% probability displacement ellipsoids and the atom numbering scheme.



Scheme 8. Synthesis of trimethyltin isonicotinate (**8**) and trimethyltin nicotinate (**9**).

The ^1H NMR spectrum, Figure 10 below, confirmed the formation of the target products **8** and **9**. In the aliphatic region, a minor change is observed to the chemical shift of the hydrogen atoms of the methyl groups in compounds **8** and **9** ($\delta_{\text{H}1} = 0.67$ and $\delta_{\text{H}1} = 0.67$ ppm, respectively) in comparison to the starting material ($\delta_{\text{H}1} = 0.65$ ppm). No signal for the protons of the methyl group of Me_3SnCl was found, indicating a total consumption of the starting material. As in the case of the previous triorganotin compounds bearing the same carboxylic groups, the signals in the aromatic region confirmed the presence of the target compounds: two signals detected for compound **8** ($\delta_{\text{H}4} = 7.85\text{--}7.86$ and $\delta_{\text{H}5} = 8.71\text{--}8.73$ ppm) and four signals recorded for **9** ($\delta_{\text{H}4} = 9.21$, $\delta_{\text{H}5} = 8.69\text{--}8.71$, $\delta_{\text{H}6} = 7.36\text{--}7.38$ and $\delta_{\text{H}7} = 8.31\text{--}8.33$ ppm).

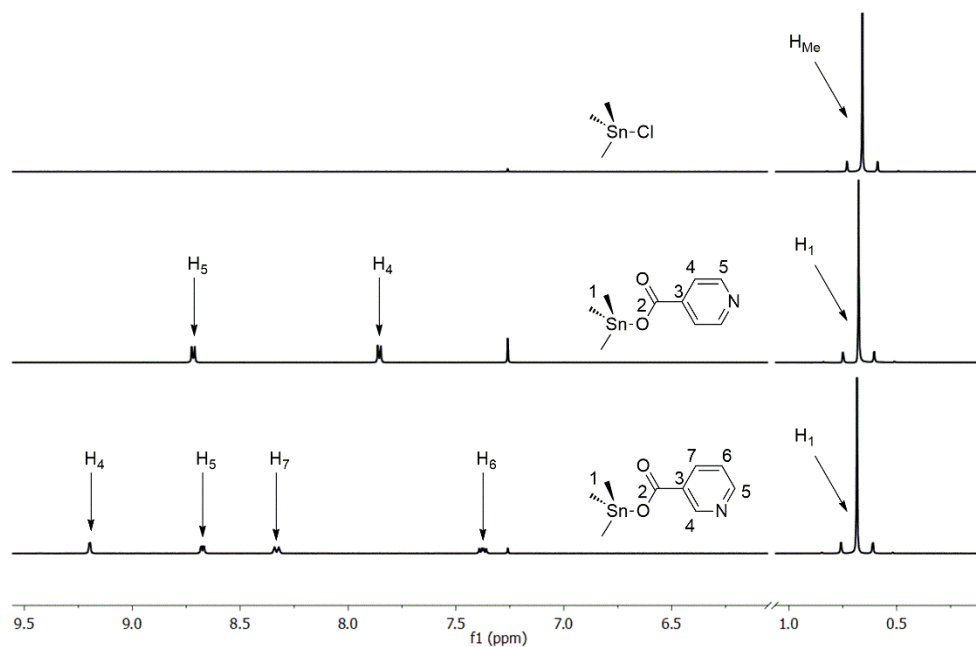


Figure 10. Details of the stacked ^1H NMR spectra (400 MHz, CDCl_3) of the starting material (top), compounds **8** (middle) and **9** (bottom).

In the ^{119}Sn NMR spectrum, a single signal was found for both compounds **8** and **9**, confirming that all starting material was consumed. After several measurements, an unexpected behavior was noticed for both compounds: The chemical shifts of **8** and **9** are concentration dependent, this behavior was more apparent in the ^{119}Sn NMR than with any other nucleus (Figures 11 and 12). This effect is well known and studied for several nuclei in NMR including ^{119}Sn .

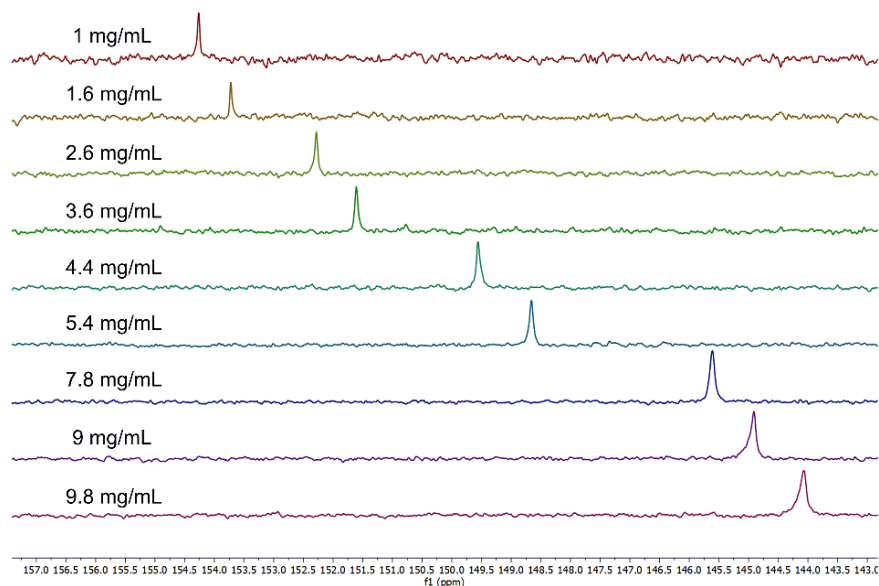


Figure 11. Stacked ^{119}Sn NMR spectra (149.2 MHz, CDCl_3) of compound **8** at different concentrations.

In the ^1H NMR, the variation of chemical shifts was most visible in the aromatic area of the ^1H NMR spectra (Figure 12). At 0.268 mg/mL: $\delta_{\text{H}4} = 9.24$ ppm, $\delta_{\text{H}5} = 8.74$ ppm, $\delta_{\text{H}6} = 7.36$ ppm and $\delta_{\text{H}7} = 8.31$ ppm, while at 81 mg/mL: $\delta_{\text{H}4} = 9.15$ ppm, $\delta_{\text{H}5} = 8.61$ ppm, $\delta_{\text{H}6} = 7.38$ ppm and $\delta_{\text{H}7} = 8.34$ ppm.

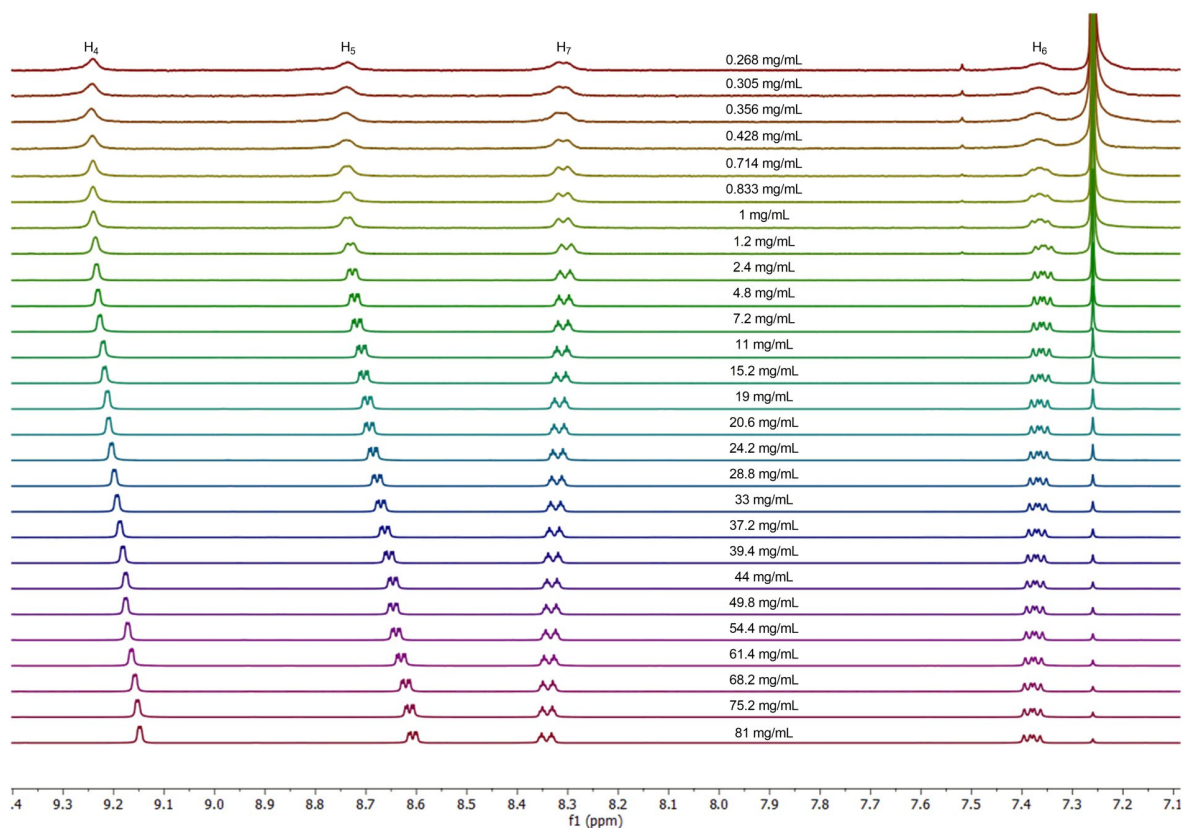


Figure 12. Stacked ¹H NMR spectra (400 MHz, CDCl₃) of the aromatic region of compound 9 at different concentrations.

In the ¹¹⁹Sn NMR spectra, as showed in Figure 13 below, by increasing the quantity from 0.134 mg to 40.5 mg, in 0.5 mL of CDCl₃, the $\delta_{119\text{Sn}}$ shifted upfield from 150.51 ppm to 89.3 ppm (all measurements performed at the same temperature). These variations show a strong linear relationship between chemical shift and concentration.

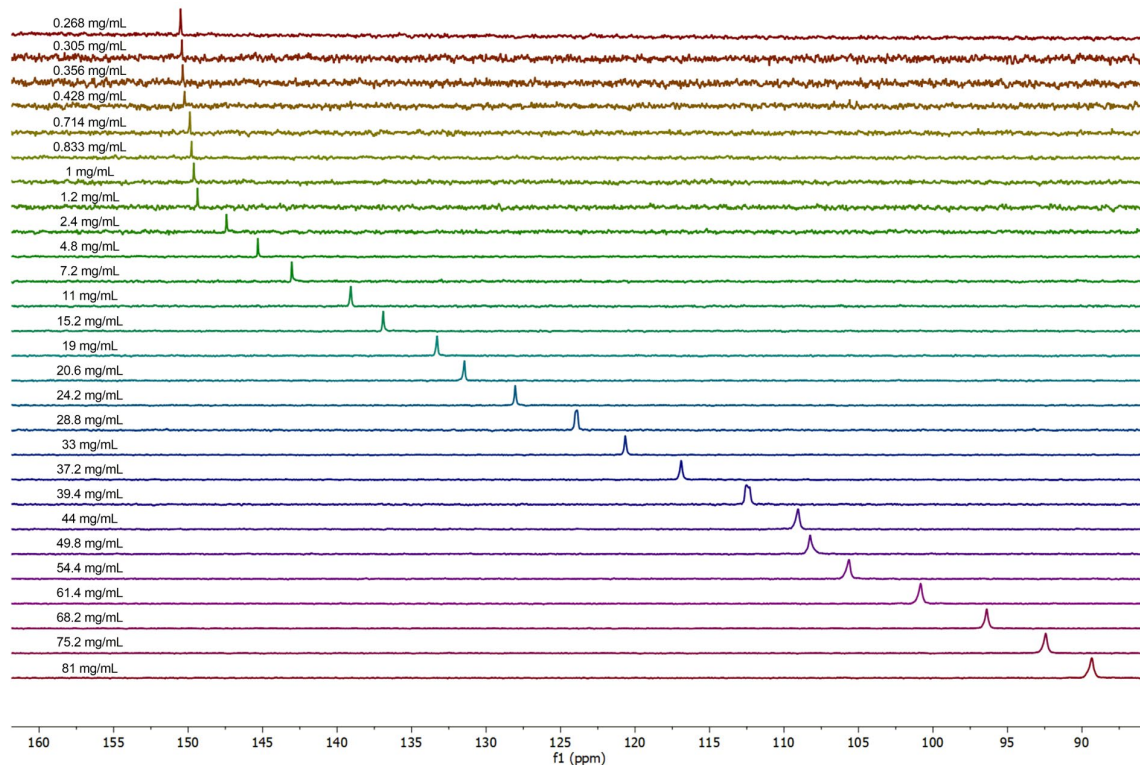


Figure 13. Stacked ^{119}Sn NMR spectra (149.2 MHz, CDCl_3) of compound **9** at different concentrations.

Beside the observed variation of chemical shifts in ^{119}Sn NMR ($\delta_{119\text{Sn}}$), the coupling constants in the ^1H and ^{13}C NMR spectra $^2J_{117/119\text{SnH}}$ and $^1J_{117/119\text{SnC}}$, respectively, were also found to change in function of concentration, with greater changes for the latter. These changes are also found to follow a relatively linear relationship between both $^1J_{117/119\text{SnC}}$, $^2J_{117/119\text{SnH}}$ and concentration as showed in graphs 14 and 15 below.

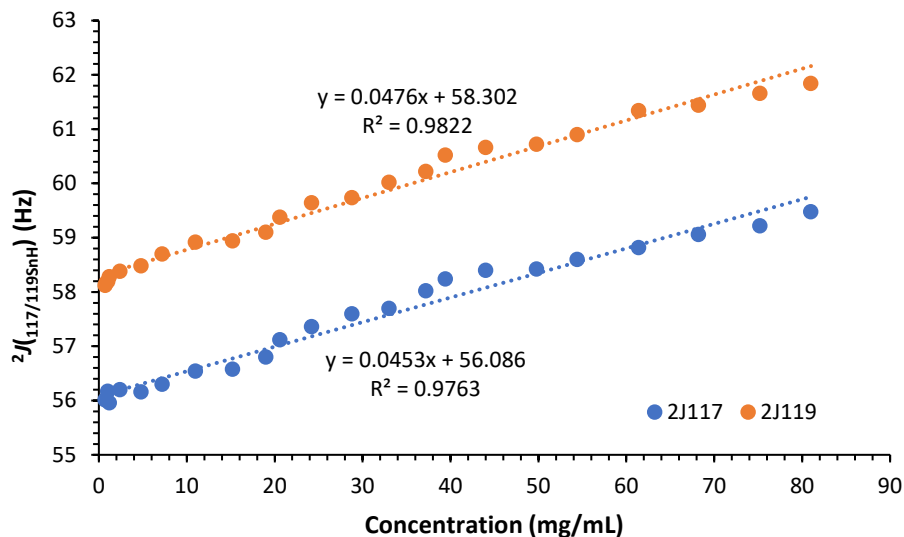


Figure 14. $^2J_{119\text{SnH}}$ and $^2J_{117\text{SnH}}$ in function of concentration.

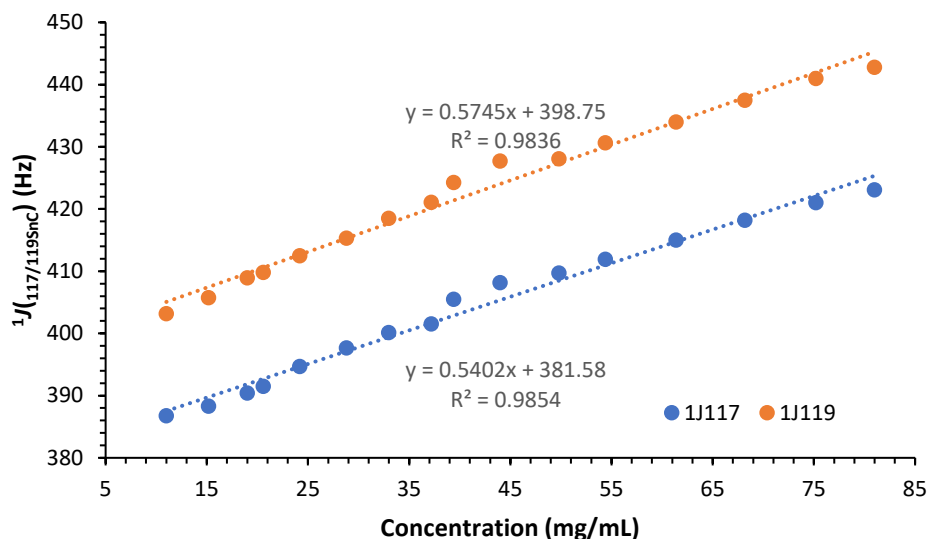


Figure 15. $^1J_{119\text{SnC}}$ and $^1J_{117\text{SnC}}$ in function of concentration.

The dynamic effects in solution for the triorganotin(IV) carboxylates discussed in this work rise a structural uncertainty. Meaning that two possible ways of oligomerization might occur, either oligomerization *via* formation of coordination bonds between the nitrogen atom from the heteroaromatic ring to the tin center or *via* anion carboxylic bridging, as showed in Figure 16 below. Both types of associations are found in literature for triorganotin(IV) carboxylates, as form of stable dimers,¹⁶ oligomers^{17,18,19} or even polymers.^{20,21} Both types of associations are not present in the same solution since only a single signal is present in ^{119}Sn NMR spectrum.

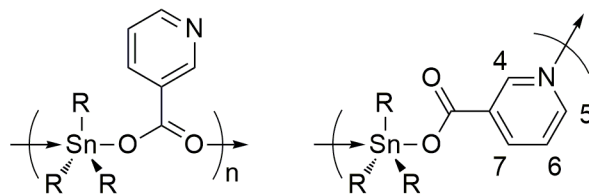


Figure 16. Possible proposed triorganotin(IV) carboxylate chain association.

¹⁶ R. Zhang, Y. Ren, Q. Wang, C. Ma, *Inorg. Chim. Acta*, **2010**, 363(7), 1597-1600.

¹⁷ H. D. Yin, M. Hong, M. L. Yang, J. C. Cui, *J. Mol. Struct.*, **2010**, 984(1-3), 383-388.

¹⁸ X. X. Gan, L. F. Tang, *J. Coord. Chem.*, **2011**, 64(14), 2458-2465.

¹⁹ Y. F. Xie, Y. Yu, Z. J. Fan, L. Ma, N. Mi, L. F. Tang, *Appl. Organomet. Chem.*, **2010**, 24(1), 1-7.

²⁰ Y. F. Win, C. S. Choong, S. G. Teoh, C. K. Quah, H. K. Fun, *Acta Cryst.*, **2011**, E67(9), m1276-m1277.

²¹ T. D. Li, H. Y. You, *Acta Cryst.*, **2007**, E63(7), m1870.

In order to elucidate which type of association takes place in solution, it is important to point out that the hydrogen atoms next to the nitrogen site of the heteroaromatic ring experience the biggest change in chemical shift in compound **9**'s ^1H NMR ($\Delta\delta_{\text{H}_4} = -0.09$ ppm and $\Delta\delta_{\text{H}_5} = -0.13$ ppm) and both are shifting upfield. A similar behavior was observed in the ^{13}C NMR for C_4 and C_5 where $\Delta\delta_{\text{C}_4} = -0.68$ ppm (between 1.2 mg/mL and 49.8 mg/mL) and $\Delta\delta_{\text{C}_5} = -1$ ppm (between 2.4 mg/mL and 49.8 mg/mL). These upfield shifts might be attributed to a higher shielding generated for H_4 and H_5 by the softening of the nitrogen's electronegativity, indicating that this donor site is likely to be involved in the intermolecular $\text{N} \rightarrow \text{Sn}$ interaction. Also, the X-ray diffraction on single crystals of these compounds revealed that they are polymeric in nature *via* $\text{Sn}-\text{N}$ coordination bonds (in solid state) and that the hydrogen atom in the *para* position (H_5) is involved in supramolecular interactions, as it will be discussed later, which might explain the reason behind the biggest $\Delta\delta_{\text{H}}$ value observed.

A series of solution and solid-state NMR studies were performed in order to correlate the coupling constant (J) and the $\text{Me}-\text{Sn}-\text{Me}$ angle (θ) leading to many proposed and used equations describing the relation between them. Lockhart and coworkers proposed the following equation: $\theta = 0.0161|{}^2J|^2 - 1.32|{}^2J| + 133.4$, ${}^2J_{119\text{SnH}}$, for compounds in solution,²² while proposing the following equation: $|{}^1J_{119\text{SnC}}| = 11.4(\theta) - 875$ for solid-state compounds.²³ With the increase of concentration, the tin atoms in an oligomeric state increase, increasing the population of tin atoms having a $\text{C}-\text{Sn}-\text{C}$ angle of 120° (trigonal bipyramidal geometry) from a previous 109° one (tetrahedral geometry). The former equation allows us to calculate the mean $\text{C}-\text{Sn}-\text{C}$ angle ($\bar{x}\theta$) of the tin atom population for compound **9** in a given concentration: from 111.06° at 11 mg/mL to 113.34° at 81 mg/mL. Graphical representations of the variation of values are shown in Figures 17 and 18 below. While using the same equation for the $\text{C}-\text{Sn}-\text{C}$ angle in DMSO: $\theta = 120.19^\circ$, which is an indicator of the adoption of an almost perfect trigonal bipyramidal geometry considering the $\text{O}_{\text{carbox}}-\text{Sn}-\text{N}$ angle to be a perfect 180° ($\tau_5 \approx 1$).

²² T. P. Lockhart, W. F. Manders, *Inorg. Chem.*, **1986**, 25(7), 892-895.

²³ T. P. Lockhart, W. F. Manders, J. J. Zuckerman, *J. Am. Chem. Soc.*, **1985**, 107(15), 4546-4547.

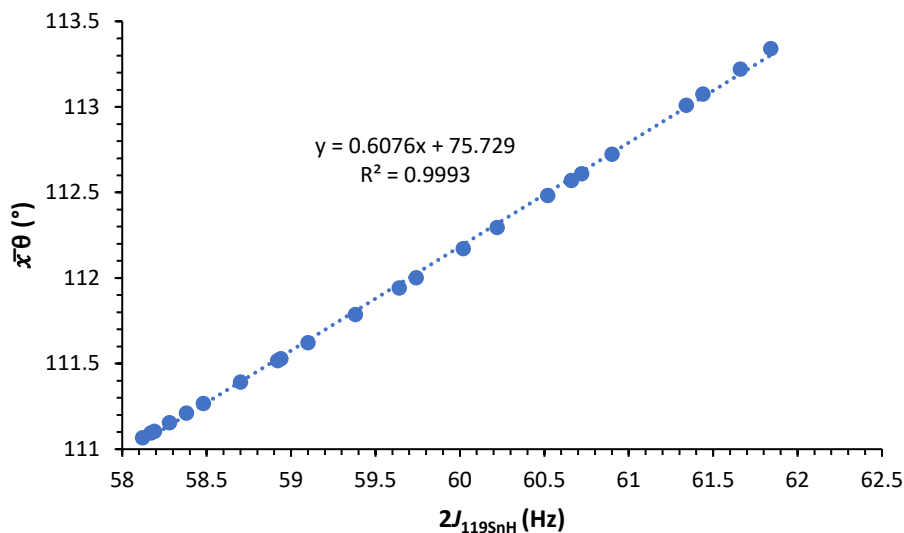


Figure 17. C–Sn–C angle $\bar{x}\theta$ in function of ${}^2J_{119\text{SnH}}$.

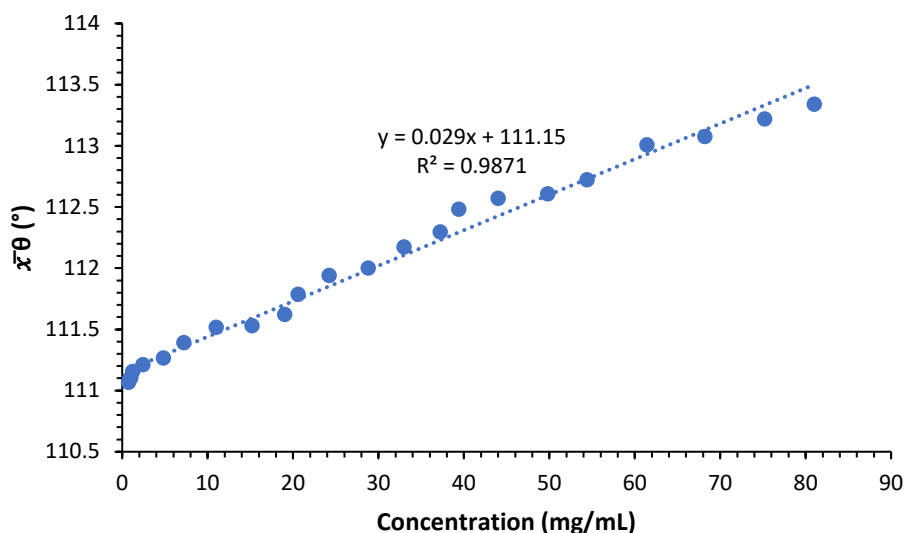


Figure 18. C–Sn–C angle $\bar{x}\theta$ in function of concentration (mg/mL).

Therefore, it is safe to assume that the type of association in solution is a polymeric one *via* Sn–N coordination rather than anion bridging one. Also, with the concentration changes, the modification of chemical shifts (δ) and coupling constants (${}^2J_{117/119\text{SnH}}$ and ${}^1J_{117/119\text{SnC}}$) found in the ${}^1\text{H}$, ${}^{13}\text{C}$ and ${}^{119}\text{Sn}$ NMR spectra are due to gradual alteration in the population of two different types of tin centers. The polymer character of the compound also increases (higher molecular mass) at higher concentrations making it more susceptible to precipitate justifying the limit of this study to 81 mg/mL.

As other triorganotin(IV) nicotines²⁴ and iso-nicotines,²⁵ both compounds **8** and **9** are found to exist in solid-state as coordination polymers *via* repetitive linked N–Sn coordination bonds.²⁶

The tin atom in compound **8** is found to be pentacoordinated and adopts a trigonal bipyramidal geometry, with a geometry index $\tau_5 = 0.879$, where the carbon atoms of the methyl groups occupy the equatorial positions while an oxygen atom from the carboxylic group occupies one apical position and a nitrogen atom from a neighboring monomer occupies the opposite apical position. The ORTEP-like diagrams are depicted respectively in Figures 19 and 20.

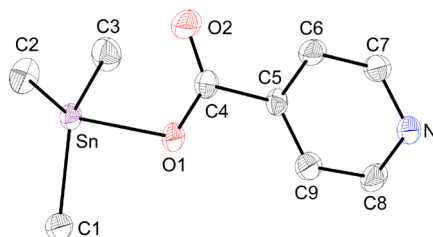


Figure 19. ORTEP representation of the molecular structure of $(\text{CH}_3)_3\text{SnO}_2\text{CC}_5\text{H}_4\text{N-4}$ (**8**) showing 30% probability displacement ellipsoids and the atom numbering scheme.

For compound **9** the geometry index of the tin center ($\tau_5 = 0.797$) indicates a trigonal bipyramidal geometry, where the carbon atoms of the methyl groups hold the equatorial positions while an oxygen atom from the carboxylic group holds one apical position and a nitrogen atom from a neighboring monomer holds the opposite apical position.

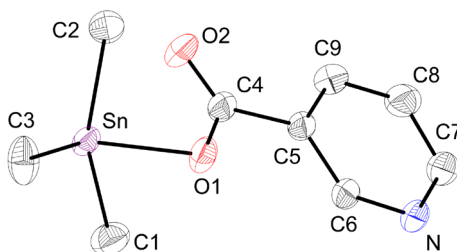


Figure 20. ORTEP representation of the molecular structure of $(\text{CH}_3)_3\text{SnO}_2\text{CC}_5\text{H}_4\text{N-3}$ (**9**) showing 30% probability displacement ellipsoids and the atom numbering scheme.

²⁴ S. W. Ng, V. G. K. Das, F. van Meurs, J. D. Schagen, L. H. Straver, *Acta Crystallogr. Sect. C: Struct. Chem.*, **1989**, 45(4), 570-572.

²⁵ H. D. Yin, C. H. Wang, Q. J. Xing, *Polyhedron*, **2004**, 23(10), 1805-1810.

²⁶ S. H. Etawi, T. A. Fayed, M. M. El-bendary, H. Marie, *Appl. Organometal. Chem.*, **2018**, 32(2), e4066.

3. Coordination polymers

3.1. General introduction

Coordination polymers are macromolecules that, as their name indicates, incorporate both aspects of polymer and coordination chemistry; having constitutional repeating units linked together *via* coordination bonds.

A deeper study and understanding of the types of supramolecular interactions between synthons leads to a better comprehension of how polymolecular networks form, which in turn improves the synthesis and the pioneering of coordination networks.

3.2. Single crystal X-ray diffraction

Reaction with AgClO₄

a. [Ag{Me₃Sb[O(O)CC₅H₄N-3]₂}(ClO₄)]·H₂O (10·H₂O)

From a solution of compound **2** in CHCl₃ reacted with a solution of AgClO₄ in EtOH in the absence of light, single crystals of [Ag{Me₃Sb[O(O)CC₅H₄N-3]₂}(ClO₄)]·H₂O suitable for X-Ray measurement were isolated. Compound **10**·H₂O crystallizes in the monoclinic space group P2₁/c. It should be noted that, while none of the solvents' molecules are participating in the supramolecular structure nor in the silver's coordination sphere, a water molecule either from the atmosphere's humidity or the EtOH is found coordinated to the silver center. Applying the geometry index for the pentacoordinated silver core: $\tau_5 = 0.06$, indicating the adoption of a square pyramidal geometry. With nitrogen atoms from the pyridyl groups filling the *trans* isomer positions in the base [N1–Ag 2.169 Å, N2'–Ag 2.176 Å] and oxygen atoms from the perchlorate anion and carboxylate group occupying the remaining two positions [O5–Ag 3.146 Å, O1A–Ag 3.285 Å], while the oxygen atom from the coordinated water fills the apical site [O9–Ag 2.629 Å]. In solid state, intra-repeating unit hydrogen bonds are found to take place between the organoantimony spacer and the perchlorate anion, where two oxygen atoms from the ClO₄⁻ anion bond to two hydrogen atoms from two different methyl groups of the organometallic spacer [O6···H1 2.547 Å, O7···H4 2.650 Å]. The counteranion also forms a hydrogen bond between an oxygen atom and an *ortho* hydrogen atom from the nicotinate moiety [O7···H10 2.478 Å, Σr_{vdw} (H,O) 2.72 Å], as showed below in Figure 21.

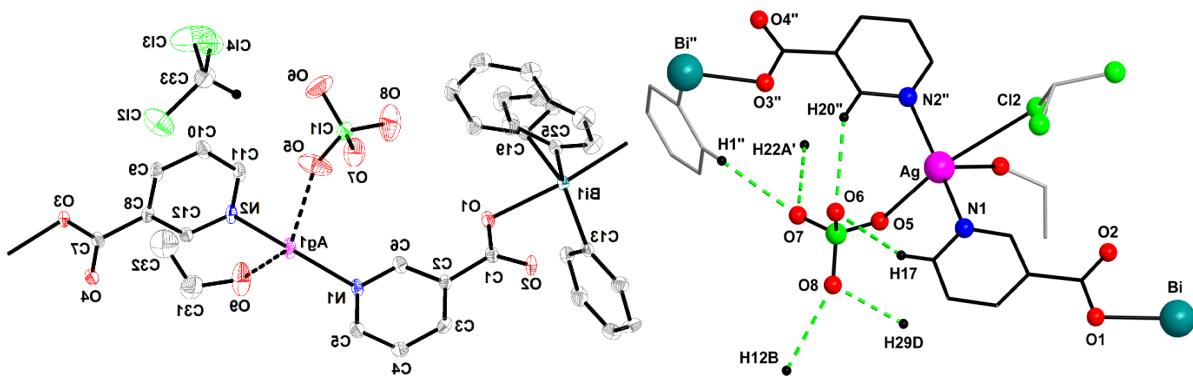


Figure 22. Constitutional repeating unit displaying solvents' intra-repeating unit interactions (left) and the perchlorate interactions (right).

The topology of the strand is described as a sawtooth like 1-D coordination polymer due to the bidentate spacer (μ_2) adopting an antiperiplanar conformation with a dihedral angle between the heteroaromatic rings = 169.9° , where the donor sites of the pyridine moieties are oriented in opposite directions (Figure 23).

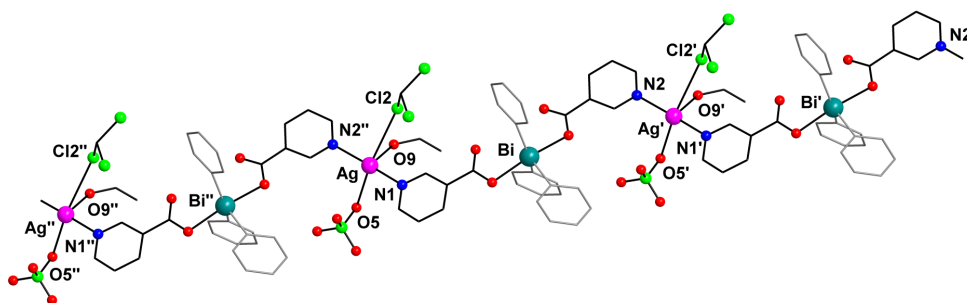


Figure 23. 1-D coordination chain, symmetry equivalent atoms are designated with ' and '' signs.

Reaction with AgOTf

a. $[\text{Ag}\{\text{Ph}_3\text{Sb}(\text{nic})_2\}(\text{OTf})]$ (**12**)

The honeycomb-like 2-D coordination polymer was obtained by reacting a solution of **3** in CHCl_3 and a solution of AgOTf in acetone in the absence of light. The silver center adopts a geometry closer to a square planar shape with a geometry index of $\tau_4 = 0.203$, where two nitrogen atoms from the linker's pyridyl rings [$\text{N1}-\text{Ag}$ 2.103 Å, $\text{N2}-\text{Ag}$ 2.142 Å] and two oxygen atoms from the triflate bridging anions [$\text{O2}-\text{Ag}$ 2.865 Å, $\text{O6A}-\text{Ag}$ 3.165 Å] adopt a *trans* configuration within the square base, as presented in Figure 24 below.

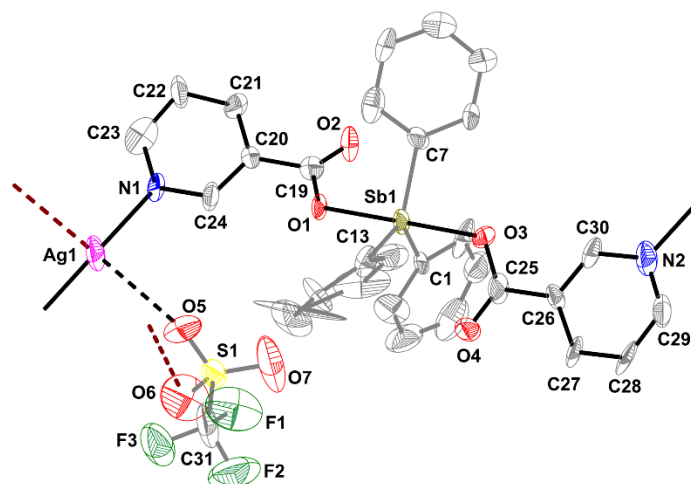


Figure 24. Repeating unit with heteroaromatic rings adopting an antiperiplanar conformation.

Several attempts were made to obtain suitable crystals for X-ray measurements yielding crystals of poor quality leading to structural irregularities such as: non planar phenyl and pyridyl groups. Substitutional disorder and disordered solvent molecules were present in the structure of the measured crystal.

In this case, a single coordination chain adopts a triangular wave-like topology. The linkers were found to adopt an antiperiplanar conformation with a dihedral angle of 164.1°.

b. [Ag{Me₃Sb[O(O)CC₅H₄N-4]₂}(OTf)]·CHCl₃ (13·CHCl₃)

This 1-D coordination polymer was obtained by reacting a solution of Me₃Sb[O(O)CC₅H₄N-4]₂ in CHCl₃ with a solution of AgOTf in acetone in the absence of light. According to the geometry index, $\tau_5 = 0.242$, the pentacoordinated silver center adopts a distorted square pyramidal geometry. The square base is formed by nitrogen atoms from the pyridyl rings [N1–Ag 2.174 Å, N2''–Ag 2.179 Å] in a *trans* configuration while the chlorine atom from the CHCl₃ solvent [Cl1–Ag 3.607 Å] and the oxygen atom from the bridging triflate [O5A–Ag 2.632 Å] filling the two remaining positions and the oxygen atom from the silver's triflate [O5–Ag 2.628 Å] holds the top of the pyramid.

The crystallization chloroform is found to form an intra-repeating unit hydrogen bond with an oxygen atom from the triflate anion [O6···H18 2.266 Å]. As expected, the triflate group is an important binding entity, where it links several chains *via* three hydrogen bonds and an anion bridging (Figure 25). Although the dihedral angle between the pyridine moiety plans = 67.6°, this does not affect the linearity of the

polymer due to the nitrogen donors being present in the *para* position of the ring, this angle could be a result of secondary interactions with neighboring chains allowing for a more stable structure.

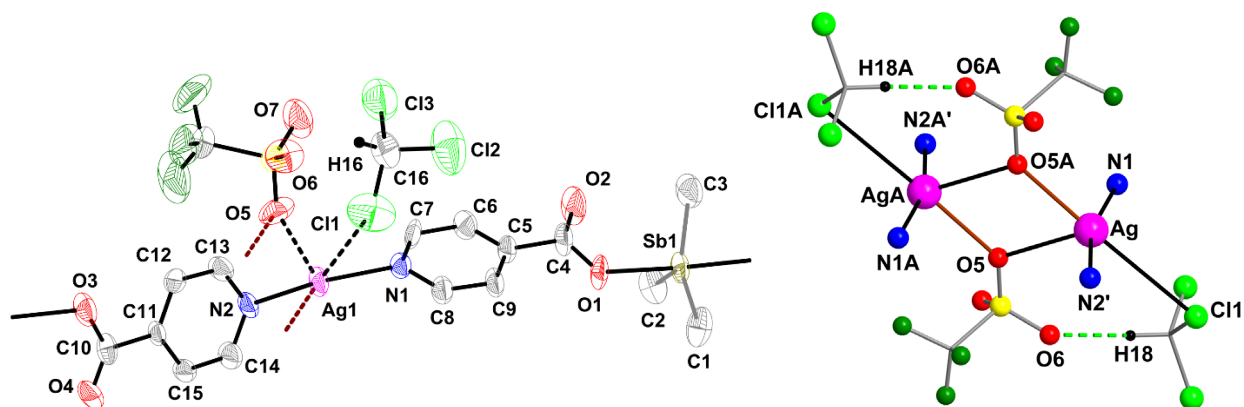


Figure 25. Repeating unit (left) and the node's anion bridging (right).

c. **[Ag{Me₃Sb[O(O)CC₅H₄N-3]₂}] (OTf) (14)**

The coordination network **14** was obtained by reacting a solution of Me₃Sb[O(O)CC₅H₄N-3]₂ in CHCl₃ and a solution of AgOTf in acetone in the absence of light. The geometry index for the pentacoordinated silver center is $\tau_5 = 0.501$ indicating that a distorted geometry adopted in between square pyramidal and trigonal bipyramidal. Two nitrogen atoms from the pyridyl groups are filling the axial positions [N1–Ag 2.144 Å, N2'–Ag 2.165 Å] while three oxygen atoms from bridging triflate anions [O5–Ag 2.79 Å, O6A'–Ag 3.007 Å, O4C–Ag 3.351 Å]. The spacer adopts an antiperiplanar conformation with a dihedral angle = 164.7°, where the donor sites are oriented in opposite directions. Despite the complexity of this compound, no intra-repeating unit secondary interactions were found.

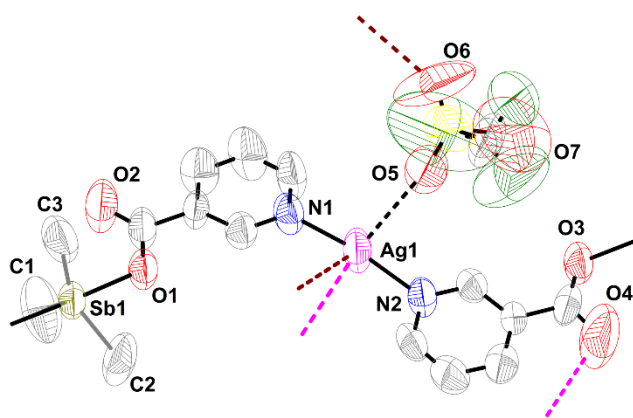


Figure 26. Repeating unit with spacer displaying polydentate character (μ_3).

The main 1-D chain consists of a sequence of repetitive spacer and node adopting a sawtooth-like shape, where two types of inter-repeating unit secondary interactions are found: two hydrogen bonds formed between an *ortho* hydrogen atom from the heteroaromatic ring and an oxygen atom from the triflate anion [H14···O5" 2.646 Å] while a hydrogen atom from the methyl group and a fluorine atom from the triflate counteranion were found to bond [H1···F1" 2.506 Å Σr_{vdW} (H,F) 2.67 Å]. The C16-F1 bond is the shortest in the trifluoromethyl moiety, a characteristic contradicting the general structural feature encountered when a halogen bond is found.²⁷

Reaction with $(\text{Ph}_3\text{P})_2\text{Cu}(\text{ClO}_4)$:

The coordination polymer **15** was obtained by reacting a solution of $\text{Me}_3\text{Sb}[\text{O}(\text{O})\text{CC}_5\text{H}_4\text{N}-4]_2$ in CHCl_3 and a solution of $\text{Cu}(\text{Ph}_3\text{P})_2(\text{ClO}_4)$ in acetone. The geometry indexes for the tetracoordinated Cu center: $\tau_4 = 0.896$ and $\tau'_4 = 0.898$, indicating the adoption of a tetrahedral geometry (Figure 27).

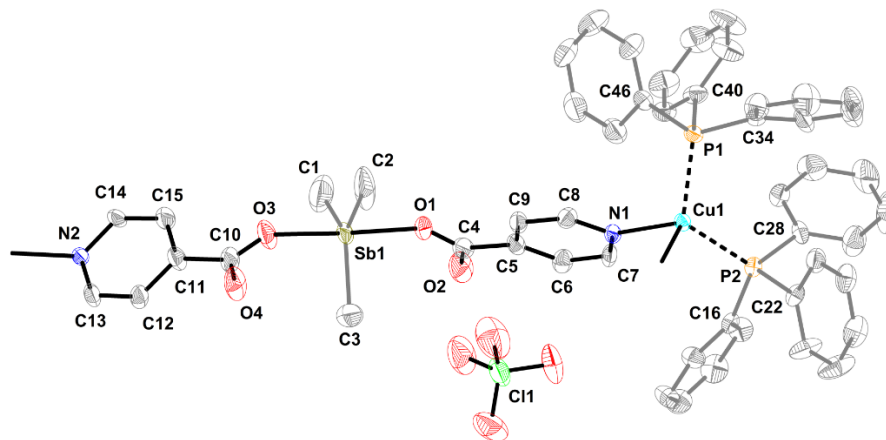


Figure 27. Repeating unit showing the ClO_4^- anion out of the metal's coordination sphere.

This type of geometry coupled with the linear nature of the spacer give rise to a 1-D coordination polymer with a triangular wave-like (zig-zag) structure. The two PPh_3 are coordinated to the metal center through their phosphorous centers [P1–Cu 2.25 Å, P2–Cu 2.25 Å] while the anion was expelled from the metal's coordination sphere due to the coordinating nitrogen atoms from the heteroaromatic rings [N1–Cu 2.099 Å, N2"–Cu 2.102 Å]. The dihedral angle between the plans of the pyridine rings = 81.2°, this didn't affect the overall topology of the network since the orientation of the donor elements is the same.

²⁷ D. M. P. Mingos, P. Metrangolo, G. Resnati, *Halogen Bonding: Fundamentals and Applications*, Springer, Milan, 2007.

Reaction with Hg(SCN)₂:

a. [Hg₃{Me₃Sb[O(O)CC₅H₄N-4]}₂](SCN)₆ (**16**)

Compound **16** was obtained as a coordination network by reacting a solution of Me₃Sb(isonicotinate)₂ in CHCl₃ with a solution of Hg(SCN)₂ in MeOH. Although the reagents were mixed in a 1:1 stoichiometry, a coordination polymer with a 2:3 ratio of spacer:node was obtained. Within a repetitive unit, two organometallic spacers are connected *via* a pair of reciprocal hydrogen bonds between methyl group hydrogen atoms and oxygen atoms from carboxylic fragments [H1...O6 and H18...O2 2.3 Å]. The node is constituted of three Hg(SCN)₂ salts bonded together *via* thiocyanate anion bridging forming two hexa atomic cycles linked in a spiro like shape with the central mercury atom acting as the defining single common atom and each of the rings adopts a distorted chair conformation (Figure 28).

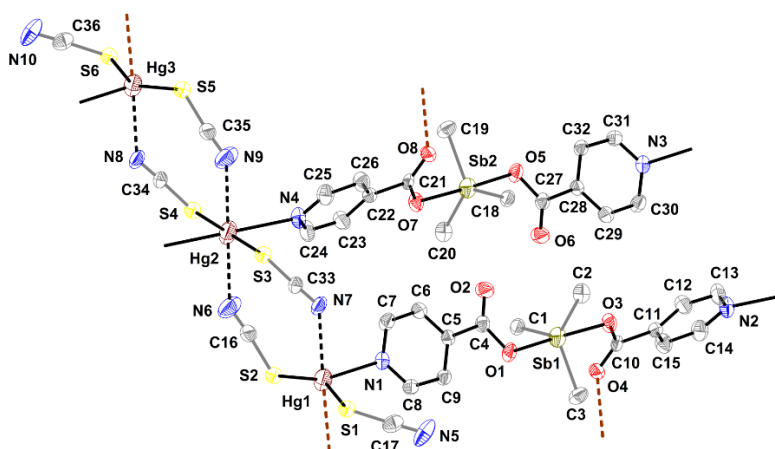


Figure 28. Repeating unit in compound **16** and its hydrogen bonds.

From these three mercury centers, the first is coordinated exclusively to the first homo-repeating unit spacer, the second mercury center is bonded to both the second homo-repeating unit spacer and the following first hetero-repeating unit spacer, while the third center is coordinated exclusively to the following second hetero-repeating unit spacer. For Hg1 and Hg3, $\tau_5 = 0.351$ which indicates the adoption of a distorted square pyramidal geometry, both centers adopt the same geometry and have the same bond length with atoms in their coordination spheres. The square base is formed by a nitrogen atom from the thiocyanate anion [N7–Hg1 and N8–Hg3 2.569 Å] and an oxygen atom from neighboring chain's carboxylic group [O8A–Hg1 and O4B–Hg3 2.847 Å] and two sulfur atoms from the thiocyanate anions [S1–Hg1 and S3–Hg3 2.402 Å, S2–Hg1 and S5–Hg3 2.4 Å] adopting a *trans* configuration while a nitrogen atom

from the coordinated heteroaromatic ring [N1–Hg1 and N3''–Hg3 2.422 Å] occupies the apical position. Meanwhile, Hg2 adopts an almost perfect (exemplary) octahedral geometry, with two sulfur atoms from the thiocyanate anion [S3–Hg2 2.429 Å, S4–Hg2 2.429 Å] and two nitrogen atoms from the pyridine groups [N4–Hg2 2.629 Å, N2''–Hg2 2.629 Å] in a *trans* configuration while the coordinating nitrogen atoms from neighboring bridging thiocyanate [N6–Hg2 2.728 Å, N9–Hg2 2.728 Å] occupying the axial positions. The dihedral angle between heteroaromatic rings of the organoantimony spacers = 67.3°, this angle is not found to affect the topology of the network.

b. **[Hg{Me₃Sb[O(O)CC₅H₄N-3]}₂](SCN)₂ (17)**

By reacting a solution of Me₃Sb(nicotinate)₂ in CHCl₃ with a solution of Hg(SCN)₂ in MeOH, a coordination polymer in the form of suitable single crystals for X-ray diffraction analysis was obtained. A peculiar aspect is observed at the repeating unit level, where consecutive mercury centers have different geometry indexes: the first having $\tau_4 = 0.799$ and $\tau'_4 = 0.87$ while the second center has a $\tau_4 = 0.838$ and $\tau'_4 = 0.896$, indicating that both adopt a tetrahedral geometry with a higher degree for the latter. In both nodes, the sulfur atoms of the thiocyanate anions [S1–Hg 2.447 Å and 2.421 Å (for the first center), S2'–Hg 2.429 Å and 2.429 Å (for the second center)] and nitrogen atoms of the spacers [N1–Hg 2.475 Å and 2.32 Å (for the first center), N2'–Hg 2.424 Å and 2.329 Å (for the second center)] occupy the corner positions, as depicted in Figure 29.

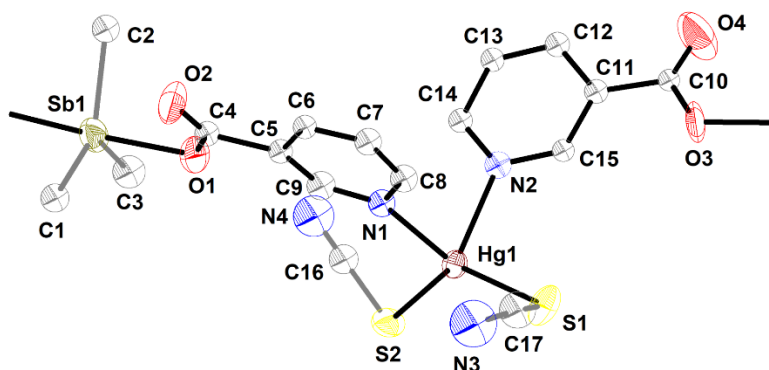


Figure 29. Repeating unit of compound **17**.

Reaction with Hg(CN)₂:

a. **[Hg{Me₃Sb[O(O)CC₅H₄N-3]}₂](CN)₂ (18)**

Suitable crystals for X-ray diffraction of compound **18** were obtained by reacting a solution of Me₃Sb(nicotinate)₂ in CHCl₃ and a solution of Hg(CN)₂ in MeOH. The polymer is found to crystallize in the

P-1 space group. The Hg node is pentacoordinated and according to the geometry index, $\tau_5 = 0.297$, the mercury center adopts a distorted square pyramidal geometry. Two carbon atoms from the cyanide anions [C16–Hg 2.062 Å, C17–Hg 2.077 Å] are in a *trans* configuration within the square plane and remaining positions are filled with two nitrogen atoms from the pyridyl moieties [N1–Hg 2.489 Å, N2''–Hg 2.543 Å] while an oxygen belonging to the carboxylate group [O4A–Hg2 3.262 Å] from the neighboring chain's spacer hold the apical position, as depicted in Figure 30 below.

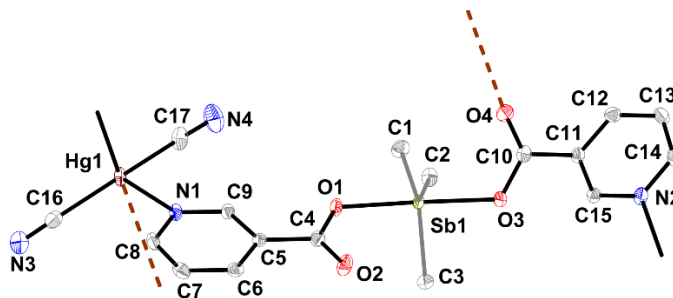


Figure 30. Repeating unit with dative bonds showed of compound **18**.

Reaction with 1,4-I₂C₆F₄:

a. $\{[\text{Me}_3\text{Sb}[\text{O}(\text{O})\text{CC}_5\text{H}_4\text{N}-3]_2] \cdot (1,4\text{-I}_2\text{C}_6\text{F}_4)\}$ (**19**)

Suitable crystals for X-ray diffraction of compound **19** were obtained after a few days of reacting a solution of Me₃Sb(nicotinate)₂ in EtOH with a solution of 1,4-I₂C₆F₄ in CH₂Cl₂. The polymer is found to crystallize in the *P*-1 space group. Both iodine atoms within a repetitive unit adopt a linear geometry, as seen in Figure 31 below, with C19–I1–N2' = 179.21° and N1–I2–C16 = 176.49°. No further intra-repetitive unit interactions found, and the solvents are not contributing in the supramolecular structure of the final product.

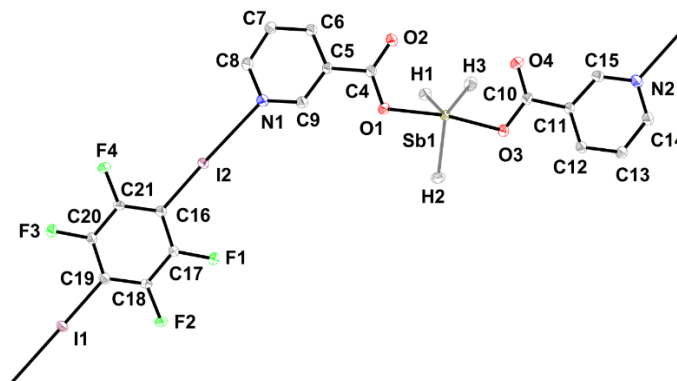


Figure 31. Repetitive unit of compound **19**.

4. Conclusion

The screening of the previously prepared triorganopnictogen(V) dicarboxylates against salts containing metals from the *d* and *p* blocks yielded nine new heterobimetallic coordination polymers **10** - **18**: two polymers **10** and **11** were obtained with AgClO₄, three polymers **12** - **14** with AgOTf, one polymer **15** with [(Ph₃P)₂Cu(ClO₄)], two polymers **16** and **17** with Hg(SCN)₂ and one polymer **18** with Hg(CN)₂. The most efficient organopnictogen tested as spacer was Me₃Sb[O(O)CC₅H₄N-3]₂ (**2**), yielding four coordination polymers.

Although the organopnictogen compounds were designed to act as bidentate spacers, they were found in many instances to be able to act in a polydentate fashion. The dimensionality of the polymers is directly influenced by the denticity of the spacers and anions bridging of the nodes. Among the obtained coordination compounds four species are 1-D coordination polymers (**11**, **13**, **15**, **17**), four are 2-D coordination polymers (**10**, **12**, **16**, **18**) and one is a 3-D coordination polymer (**14**). The effect of counter anions, solvents and orientation of the donor sites in the pyridyl moiety were described.

The screening also showed that a metathesis reaction can occur between the proposed candidate spacers and several salts containing metals from the *d* and *p* blocks. Reactions between spacers **4** and **5** and Me₃SnCl serendipitously yielded compounds **8** and **9** and the Ph₃BiCl₂ precursor that were identified *via* multinuclear NMR spectroscopy and X-ray diffraction analysis. The reaction between spacers **3-5** and Ni[S₂P(OⁱPr)₂]₂ also underwent the metathesis reaction pathway followed by redox reaction yielding triphenylpnictogens and the respective disulfide compound that were identified *via* multinuclear NMR spectroscopy. Reactions between **4** and **5** and the salts [Zn(ClO₄)₂], Co[(OCCF₃)₂CH]₂ and AgBF₄ yielded ligand exchange reaction by-products that were exclusively identified via X-ray diffraction analysis.

We observed and studied a variety of secondary interactions when spacer **2** was reacted with 1,4-I₂C₆F₄, yielding a new polymer confirming the ability of the spacer forming σ -hole chains. It is however expected that all these triorganopnictogen(V) dicarboxylate spacers can achieve similar type of polymerization.

All reactions, whether following desired reaction pathways or not, show that compounds **1** - **5** can be used as building blocks for coordination polymer chemistry but side reactions may occur. Suggesting a versatile reactivity of such compounds putting in evidence that a more cautious selection of the node is a key factor in the determination and success of the outcome product. Due to the relatively low oxophilicity of the Sb and Bi elements, the results indicate that the usage of less oxophilic metals within the nodes are

the leading choices to avoid a metathesis reaction (undesired reaction). The choice of the node's metal might not be the only factor influencing the chemical behavior; as observed the variation of the anion might also yield different reactions (Figures 107 and 108).

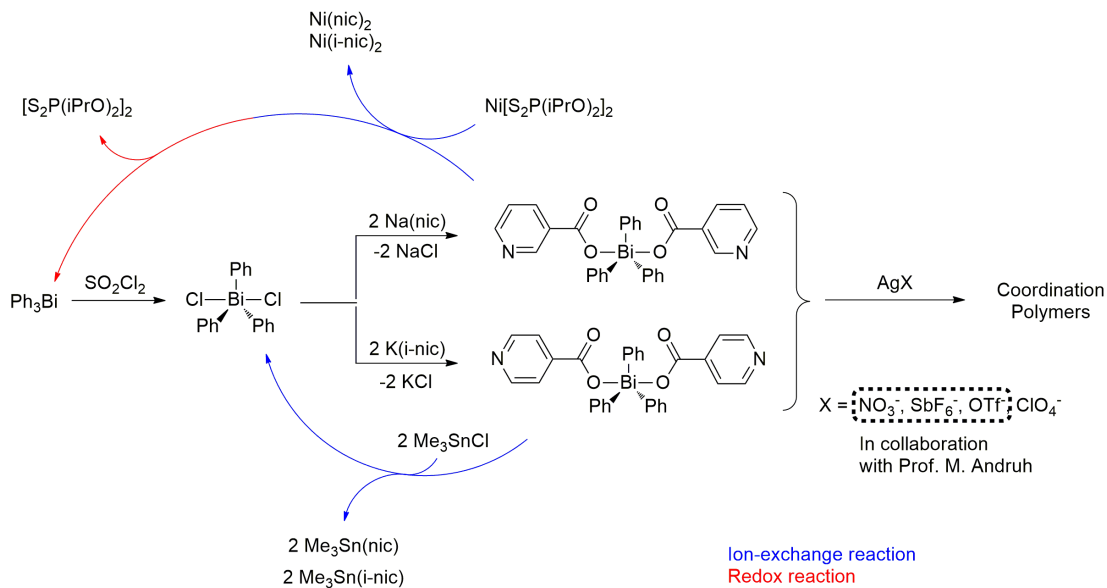


Figure 107. Reactivity chart indicating the chemical behavior of **4** and **5**.

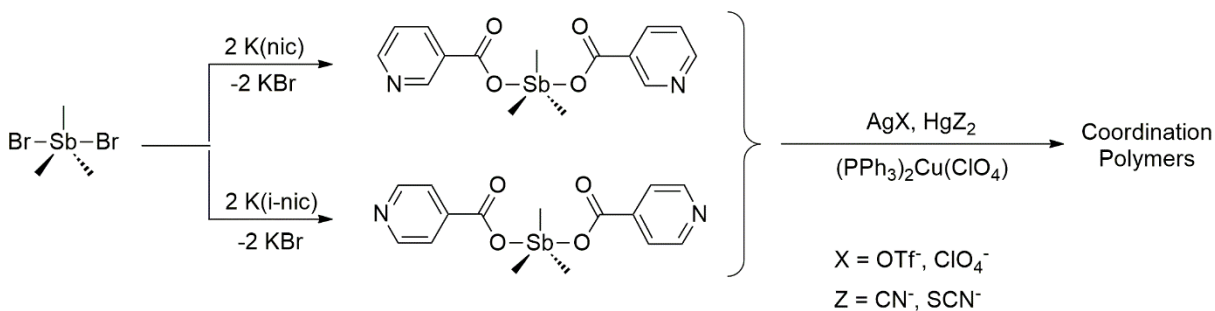


Figure 108. Reactivity chart indicating the chemical behavior of **6** and **7**.